Analysis of the failure mechanisms of a weak rock through photogrammetrical measurements

A. M. Ferrero[1], M. Migliazza[1], R. Roncella[1] and G. Tebaldi[1]
[1] Dept of Civil Engineering - University of Parma, annamaria.ferrero@unipr.it

ABSTRACT. *This research has been dedicated to the experimental study of a French Pleistocene marl through uniaxial compressive tests on prismatic specimens. Induced deformations were measured during testing by classical extensometers applied on the rock surface and by means of photogrammetrical measurements. The choice of this material was forced by its relative good characteristics in terms of material homogeneity when compared with other kinds of marl. The specimen shape was dictated by the necessity to induce plane deformation during testing to be measured by using optical methods. Specific software, implementing a correlation algorithm able to track high deformation fields and model crack propagation was developed and applied to determine displacement and deformation maps at each photogram on the whole specimen surface. Photogrammetrical method has been validated by the comparison with classical extensometer results. This measurement tool has been specifically dedicated to the identification of the microcrack formation during the performed tests for a better understanding of weak rock triggering failure phase before crack propagation start. The interpretation of experimental tests on the light of material physical and mechanical features is illustrated in the paper together with all difficulties encountered in the specimen's preparation phases due to the material peculiar nature.*

INTRODUCTION

Weak rocks and hard soils are traditionally defined as material showing a mechanical behaviour in between those associated with classical soils and rocks [1, 2]. They often show a complex mechanical behaviour mostly not uniform and anisotropic due to the presence of defects or pre-existing discontinuities, they are strongly influenced by the load law and by the deformation rate, by water content etc...[3, 8]. Moreover classical experimental devices applied for soil and rocks are often unable to test these kinds of materials for the unusual range of strength and deformability involved [9, 10]. Consequently, specific laboratory instrumentations need to be used and unconventional experimental tools to be utilised to measure stress – strain behaviour of these materials [11, 12].

In particular, the local evaluation of the strain induced by the acting stress can not be easily done by conventionally system like extensimeter since they do not guarantee a perfect cohesion with the rock surface at increasing loads. On the other hand, the failure mechanism of this material is characterised by strain localization [13, 14] even for loads

far from the ultimate one. This strain localisation are, possibly, the witness of a material damage that occurs long before the specimen collapse. The identification and the study of this phenomenon are important to quantify the material soundness at increasing acting stress.

EXPERIMENTAL WORK

Tested Material

The material chosen for this experimental work is marl denominated Beaucaire marl originally located in the South East of France in Provence. This material is already been the object of several experimental studies [15] due to its relatively homogeneous characteristics and to the possibility to acquired blocks of rock at a quarry face.

By the geological point of view, Beaucaire marl is a weak rock deposited in a sea environment during the Plio Pleistocene time. It's grey marl with fine grain, not fissured with small sand inclusions.

By a gronulometric point of view, it's characterised by 30% of clay material, by 67% of silt and by 2.7% of sand. Attenberg limits have been determined on clay fraction showing a plasticity index IP equal 15, a plasticity limit of 25% and a liquid limit of 38%. Considering the Unified Classification system Beaucaire marl can be classified as ML (inorganic silt). Its carbonate content is around 33.7%.

By a mineralogical point of view, Beaucaire marl is characterised by the presence of detritic element with random orientation and non cemented. Main minerals are calcite, feldspatic mineral, quartz and mica. In particular the marl is composed by 30% of phyllosilicate, 30% of carbonate and 30% of quartz.

Test Setup

Tests have been carry on by using a MTS-810 in a deformation rate control ($v = 2{,}08 \times 10^{-4}$ mm/s). the experimental apparatus is equipped with a load cell range ±25 kN, precision ±0.004%, whilst axial displacement are measured by a LVDT with a range of ±50 mm and a maximum error of 0.126% of full scale range.

The main problem considered in the test setup was the load axiality. In order to have a uniaxial compression state of stress the axis of the acting load must coincide with the vertical axis that pass through the specimen barycentre. Consequently the correction of the not perfect parallelism of specimens was necessary by a specific test setup. This problem was overcome by two load applicator plates connected with spherical joints (Figure 1a). This system permitted a load application able to create a simple compression acting stress in every test.

Uniaxial Compressive Tests

Ten uniaxial compressive tests have been performed at DICATeA Laboratory in Parma on prismatic specimens.

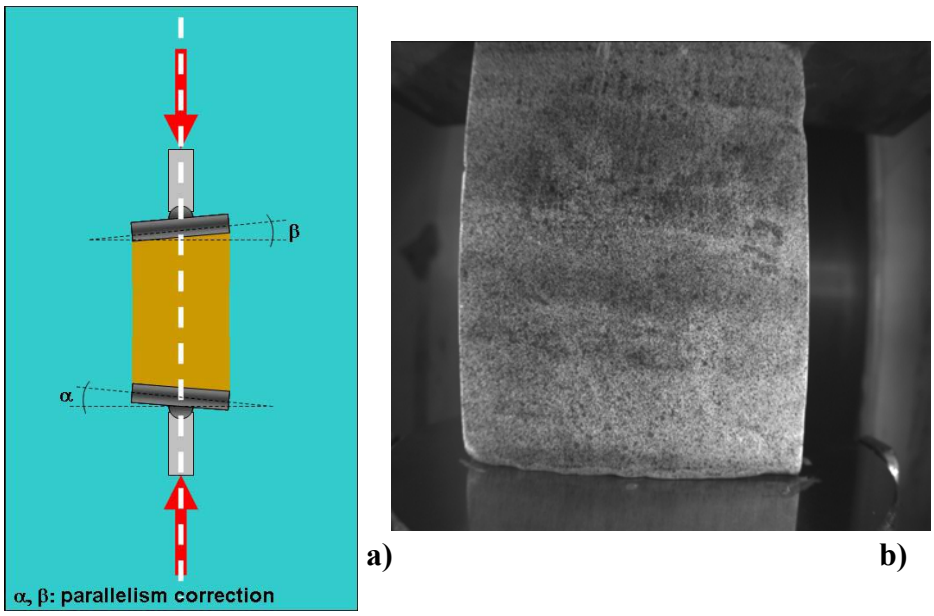

Figure 1. Load cell set up (a) and a specimen colured (b).

Specimens have been obtained by the same rock block by taking the sedimentation plane orientation into account. Specimens have been realised in such a way that uniaxial compressive axis could be maintained orthogonal to the sedimentation planes for all specimens.

Specimens have been equipped by strain gauges glue on one specimen's side by two part glue (HBM X60). Since the strain gauges could not be conveniently glued on the marl specimen surfaces, several tests have been performed in order to study the effects of the heat due to the gauges welding to the electric cables, to the heat due to the lighting system and to the marl powder present on all marl surfaces. After all these evaluation a glue density and thickness together with a welding system able to guarantee the gauges adhesion has been identified.

The specimens have also been prepared for the photogrammetrical digital measurements. Since the photogrammetrical method is based on an image correlation system, as described in following chapter, characteristic points need to be identified on the specimen surfaces. Since Beaucaire marl is nearly a homogeneous grey material, it needed to be painted in order to define identifiable points by the automatic system. Consequently specimens have been painted using black and white paints as shown in Figure 1b.

Specimens are characterised by two different sizes: larger specimens of 140x91x91 mm and smaller specimens of 75x68x25 mm.

The specimen shapes (prismatic) has been chosen to guarantee a plane surface needed for the photogrammetrical measurements. During the tests the larger specimen dimension has placed parallel to the loading axis while smaller or larger face have been measured alternatively. Strain gauges where placed on the opposite faces with respect of the face measured by the photogrammetrical method.

Photogrammetrical Method

Optical methods have become fairly widespread tools in experimental strain analysis and are especially useful when a full-field capability is required. Different moiré methods are available and have been used to measure in-plane displacements [16]. Nevertheless, if extreme accuracy in strain analysis is not an issue, digital image correlation systems provide good results at lower costs. During the last few years an image analysis software, has been developed at the University of Parma [17], to obtain indirect measurements of displacement and strain fields. The system is capable of describing in detail the strain field development of different specimen shapes and configurations, computing the displacements of the nodes of a virtual grid materialized on the specimen surface.

A digital camera (Basler Af101) was used for acquiring descriptive frames of the specimen. A 8 mm focal optics was considered adequate for the test conditions. The camera, directly connected with a PC, can acquire images at the maximum resolution allowed of 1300x1030 pixel with a frame rate of 12 fps. Since the load transmission speed on the specimen was very slow, a lower rate (1 frame every 5÷10 seconds) was used.

To obtain the highest accuracy during the image analysis process, optimal acquiring conditions must be provided. Specimen surface should be suitably painted to present a uniform, high contrasted texture. Proper lighting condition is necessary to guarantee a correct illumination of the scene and get around undesired reflexes. Finally, using only one camera to depict the plane strain field, special attention is required to limit perspective reconstruction inaccuracy during displacement evaluation. Thus, it must be ensured that the planar surface of the specimen is unable to move toward/backward from the camera. Displacements field is tracked using an Adaptive Least Square Matching (ALSM) based algorithm [18]. Although ALSM algorithms are little known and hard to implement, their use is recommended since, using a more complete functional model compared to other techniques (NCC, etc.), it is capable of high accuracy, especially with greater deformation.

The capability of the method was tested by means of different experimental investigations to evaluate the real measurements precision [17]: camera vibration, perspective correction inaccuracy, optics distortion and sensor noise are taken into account. Actually, the developed ALSM image correlation achieve accuracy of about 1/100 pixel in terms of displacement.

Precision in terms of strain estimation depends on the number of displacement nodes used during processing, or better on their interdistances Δx:

$$\begin{cases} \varepsilon_{xx}, \varepsilon_{yy} \Rightarrow \sigma_{\varepsilon} = \dfrac{\sqrt{2}}{\Delta x} \cdot \sigma_{u} \\ \varepsilon_{xy} \Rightarrow \sigma_{\varepsilon} = \dfrac{1}{\Delta x} \cdot \sigma_{u} \end{cases} \tag{1}$$

where σ_u is the estimated displacement accuracy. Assuming σ_u = 1/100 pixel and using a 40 pixel grid-step size (correspondent to more than 800 measurement nodes), precision of about 0.3÷0.5 ‰ may be expected.

EXPERIMENTAL RESULTS

Stress strain curves

Uniaxial compressive tests have supplied the stress strain curves with the strain values evaluated in 3 different ways: by means of the LVDT supplied by the MTS device system, by the photogrammetrical method and by the extensimeters. Figure 2 shows the stress strain curves obtained by the LVDT (Figure 2a) and by the photogrammetrical method (Figure 2b). Unfortunately extensimeter measurements are not reliable since the extensometer detached at low acting load except during a single test (denominated Beau 10). In this case the stress – strain curve resulting from the extensimeter measurement shows a good agreement with the same curve obtained by the photogrammetrical method. Elastic modulus and Poisson ratio at the 50% of the ultimate load has been computed for both series of curves obtaining the following results:

$$\sigma_r = 1206 \pm 101 \text{ kPa}$$

$$\varepsilon_{fotog} = 1{,}25 \pm 0{,}19\ \% \qquad E_{tfotog} = 169 \pm 47 \text{ MPa}$$

$$\varepsilon_{MTS} = 1{,}88 \pm 0{,}45\ \% \qquad E_{tMTS} = 120 \pm 34 \text{MPa}$$

where: σr is the uniaxial compressive strength, ε is the deformation at failure and E is the tangential elastic modulus at 50% of σr. The specimen water content at failure was 11%.

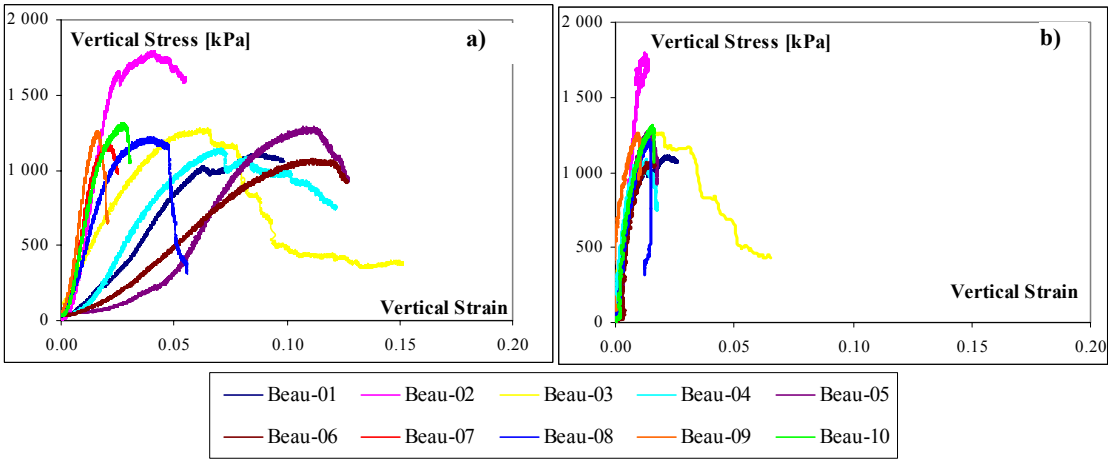

Figure 2. Stress-strain experimental curves obtained by: a) LVDT measures and b) photogrammetrical method.

These results are showing the large difference in measuring the strain value by local measurements (photogrammetrical method) in comparison with external one (LVDT). This fact due to the deformation of the system included in the external measurement system. However, the ratio between the elastic modulus and the ultimate rock strength is around 100, much lower then usual values obtained with hard rock that are usual around 200-250. This fact has been analysed in the following chapter at the light of the deformation map results.

Table 1. Maps of vertical and horizontal displacement (δy, δx), vertical and horizontal deformation (εy, εx) and photos of specimen obtained by photogrammetrical method at different load level.

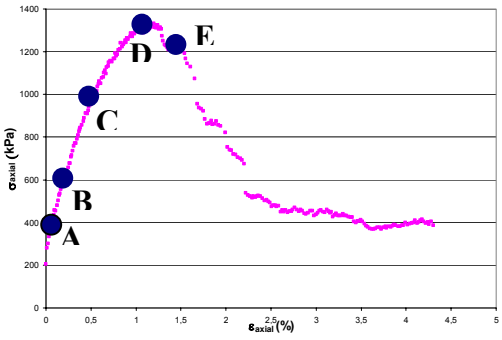

	A	B	C	D	E
δy [mm]	0 / 0.034	0 / -0.3	0 / -0.6	0 / -0.6	0 / -0.15
δx [mm]	-0.15 / -0.034	0.034 / -0.034	0.09 / -0.09	0.12 / -0.12	-1.2 / -0.15
εy [%]	0 / -0.5	0 / -1.0	0 / -1.0	0 / -2.0	2.0 / -6.0
εx [%]	0.5 / 0	0.1 / 0	0.6 / 0	1.0 / 0	2.0 / -1.0
			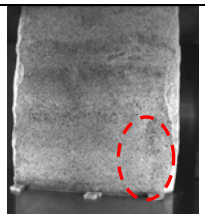	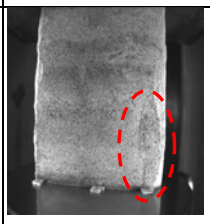	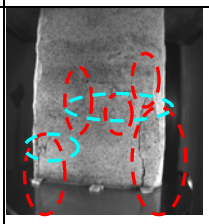

Displacement and deformation maps

As above described the photogrammetrical method also allows the determination of displacement and deformation maps that have been very useful for a better understanding of the marl failure mechanism. Table 1 reports results obtained for the specimen denominated Beau03. In this table vertical (δy) and horizontal (δx) displacement maps, vertical (εy) and horizontal (εx) deformation maps and the sample photo, obtained by photogrammetrical method at different level load are reported. Displacement maps show as the distribution of the vertical component of displacement has a sub horizontal stripe distribution due to the uniaxial condition test configuration. A non perfectly regular stripes figure at the specimen boundary can be due to the plate contact influence. The plate influence is more evident in the horizontal displacement maps where a quasi axial symmetrical distribution is shown but major displacement are measured at the specimen centre due to the friction confinement action of the specimen at the plate boundary. Strain maps are homogeneous at low applied load while they show failure localization at higher loads.

Beau03 failure is determined by both horizontal and sub vertical fracture. In this case both, horizontal and vertical strain map are useful for the failure mechanism analysis: horizontal strain maps are more useful to study vertical crack propagation while vertical strain maps show better horizontal crack development.

Strain maps allow outlining as strain localization starts at low acting stress determining non uniform strain maps at 30% of the ultimate load showing as material damage starts in correspondence with strain localisation. Rock damage at low acting loads is one possible cause of the described anomalous ratio between computed Young modulus and the ultimate rock strength.

CONCLUDING REMARKS

This work has been dedicated to experimental testing on Beaucaire marl by simple uniaxial compressive tests by using an innovative measurement system supplied by photogrammetrical techniques.

This procedure appears particularly appealing for this material where traditional extensimeter are not able to perform in a reliable way. Photogrammetrical tool gives reliable results in terms of stress strain curves and, moreover, useful information in terms of deformation and strain maps for a better understanding of the failure mechanisms. Material damage is evident in term of strain localization starting at acting loads around the 30% of the failure load and developing toward fracture maps that are coherent with the fracture pattern of the specimens at failure. Cracks are not directly observable until maximum load is reached as confirmed by the direct analysis of the photographs.

Depending on the failure crack geometry that can be characterized by vertical or horizontal main fractures strain vertical or horizontal strain component maps can be more relevant for the failure mechanism understanding.

REFERENCES

1. Morgenstern and Eigenbrod (1974) *Classification of argillaceous soils and rocks*, J. Geotech. Eng. Div. ASCE 100, GT 10 pp. 1137-1156.
2. Rutledge and Preston (1978) *Experience with engineering classification for rock*, Proc. Int. Tunnelling Symposium, Tokio, A3.1-A3.7.
3. Bescond, B. and Serratrice, J.F. (1987) *Comportement mecanique d'une marne en compression et en extension.* Rapporto AER 1 06 53 3, LRPC d'Aix In Provenza.
4. Clayton, C.R.I. and Serratrice, J.F. (1993) *Les propriétés mecaniques et le comportement des sols indures et des roches tendres*. Proc. Int. Symp. On Hard Soil And Soft Rocks, Athènes. Rapport Général Session 2.
5. Dobereiner and De Freitas (1986) *Geotechnical properties of weak sandstones*, Geotechnique, vol. 36 (1) pp. 79-94.
6. Serratrice, J.F. (1978) *Contribution a l'ètude du comportement mécanique des marnes*. Thèse D.I., IMG Université De Grenoble.
7. Serratrice, J.F. (1991) *Étude du comportement mécanique d'une argile compactée*, A62, Remblai Au PK 189, Rapport 51.44665.43, LRPC d'Aix In Provenza.
8. Serratrice, J.F. (1992) *Étude du comportement mécanique d'une craie compactée*, St Gibrien A26, Rapport 51.6194.43, LRPC d'Aix In Provenza.
9. Peels and Ferry (1983) *Needless stringency in sample preparation standards for laboratori testing of weak rocks*, Proc. 5th Congr. ISRM; Melbourne; Vol. 1 pp. 203-207.
10. Barla, G., Forlati and Zaninetti (1990) *Prove Di Laboratorio Su Rocce Tenere,* Problematiche ed Esempi, MIR, Torino.
11. Crivelli, Devin, Rossi and Superbo (1990) *Prove e misure in sito su rocce tenere*, MIR Torino.
12. Chiu, Johnston and Donald (1983) *Appropriate techniques for triaxial testing of soft rock*, Int. J. Of Rock Mech. Min.Sci.Geomech Astr; Vol.20 (3), pp. 107-120.
13. Viggiani, G., Kuntz, M. And Desrues, J. (2001) *An eperimental investigation of the relation between grain size distribution and shear banding* – Continuous And Discontinuous Modelling Of Cohesive Frictional Materials, P.A. Vermeer Et Al. Ed., pp 111-127.
14. Tamagnigni, C. And Viggiani G. (2002) *Some remarks on shear band analysis in hypoplasticity* – Localization And Bifurcation Theory For Soils And Rocks, H.B. Muhlhaus Editor, Balkema.
15. Marello S. (2004) *Comportement mécanique des roches tenders* - Politecnico Di Torino, Ph.D Thesis.
16. Siebert Th., El-Ratal W., Wegner R., Ettemeyer A. (2002) *Combine Simulation and Experiment in Automotive Testing with ESPI Measurement* – Experimental Techniques.
17. Roncella, R., Romeo E., Forlani G. (2005) Image Based Microstructural Analysis in Fracture Mechanics. *Optical 3-D Measurement Techniques*, Vol II pp. 51-60.
18. Gruen, A. (1985) *Adaptive least squares correlation*. South African Journal of Photogrammetry, Remote Sensing and Cartography, 14 (3).